IOPscience iopscience.iop.org

Home Search Collections Journals About Contact us My IOPscience

Extended defects in GaN films grown at high growth rate

This article has been downloaded from IOPscience. Please scroll down to see the full text article.

2002 J. Phys.: Condens. Matter 14 13269

(http://iopscience.iop.org/0953-8984/14/48/377)

View the table of contents for this issue, or go to the journal homepage for more

Download details:
IP Address: 171.66.16.97
The article was downloaded on 18/05/2010 at 19:17

Please note that terms and conditions apply.

INSTITUTE OF PHYSICS PUBLISHING JOURNAL OF PHYSICS: CONDENSED MATTER

J. Phys.: Condens. Matter **14** (2002) 13269–13275 PII: S0953-8984(02)53994-1

Extended defects in GaN films grown at high growth rate

E Valcheva[1], **T Paskova**[2] **and B Monemar**[2]

[1] Faculty of Physics, Sofia University, 5, J Bourchier Blvd, 1164 Sofia, Bulgaria
[2] Department of Physics and Measurement Technology, Linköping University, S-581 83 Linköping, Sweden

Received 27 September 2002
Published 22 November 2002
Online at stacks.iop.org/JPhysCM/14/13269

Abstract

A description of the present knowledge of the layer microstructure typical for thick GaN films grown at high growth rates is presented. The GaN layers are grown by hydride vapour phase epitaxy on sapphire and different buffers are used. The variety of extended defects present in such highly mismatched system are summarized, with the emphasis on their impact on the crystal quality. The defects are reviewed in two main categories according to the microstructural development during growth: large-scale nonuniformities and microstructural crystallographic defects. The first category comprises three-dimensional structural features developed mainly in the interface region, while the second are typical extended defects, i.e., dislocations with different Burgers vectors, nanopipes, inversion domain boundaries and stacking faults. The quality of the layers was improved vastly as a consequence of our understanding of the correlation of growth parameters and microstructure.

1. Introduction

The growth of bulk GaN single crystals, as e.g. obtained from melt solution at high pressure or by the sublimation technique, remains limited by scale problems. The GaN technology still relies on heteroepitaxial growth, and due to the high mismatch between the nitrides and all available foreign substrates, the GaN layers contain a variety of structural defects [1]. Hydride vapour phase epitaxy (HVPE) has attracted great attention, mainly due to its ability to produce thick layers of high optical quality at high growth rates and low cost. The method is a promising approach for growing thick GaN films of good crystalline quality over two-inch wafers. Despite the much improved structural and optical properties of the HVPE-GaN film demonstrated, there are still many unsolved, questionable and controversial issues. In particular, the main formation mechanisms of the defects, the nature of most of the defects as well as their distribution and influence on the physical properties require further investigations. A systematic study of the origin and the evolution of the defects is needed for finding solutions for the defect density reduction and better control of the growth process.

 © 2002 IOP Publishing Ltd Printed in the UK

In this work we report on the extended defects observed in thick HVPE-GaN layers grown at high growth rate, aiming to gain insight into their nucleation and evolution. The layers are grown directly on sapphire, or utilizing different buffers, such as metal–organic chemical vapour deposited (MOCVD-) GaN templates and AlN. The defect structure was studied by using different transmission electron microscopy (TEM) techniques including diffraction contrast analysis, multiple-dark-field imaging and high-resolution transmission electron microscopy (HRTEM) in cross-sectional view and plan view.

2. Experimental details

The GaN material studied in this work was heteroepitaxially grown at $\sim$1080 °C. The samples were grown in a horizontal HVPE reactor either directly on sapphire or using high-temperature buffers. The growth rates are 1–2 μm min^{-1}. Two main types of buffer have been explored: AlN layers produced by low-energy ion-assisted reactively sputtering in a UHV sputtering system using pure N_2 as the working gas at a substrate temperature of $\sim$1000 °C; and GaN buffers, undoped and Si doped, grown by MOCVD. The AlN buffer layer thickness was varied between 500 and 1000 Å while the thickness of the GaN templates was kept at about 2.5 μm. The thickness of the main HVPE-GaN layers was varied from 10 to 150 μm. The growth details and some physical properties of these layers were published previously [2].

The microstructure of the films was studied by TEM and HRTEM using a Philips CM20 UT transmission electron microscope operated at 200 kV with a LaB_6 filament. The samples for TEM analysis were prepared in cross-sectional view and plan view by a conventional procedure including mechanical polishing followed by low-angle and low-energy ion milling to electron transparency. The structure of the layers was also examined using cross-sectional specimens by low-temperature cathodoluminescence (CL) imaging. A Gemini 1550 Leo electron microscope was used, equipped with a MONO-CL Oxford Instruments attachment.

3. Large-scale GaN/sapphire interface defects

These are three-dimensional (3D) structural features developed mainly in the interface region. In order to visualize them a panchromatic CL image in cross-section is shown in figure 1(a). A bright layer built up from individual columnar structures is clearly visible near the film–substrate interface. The upper zone of the films, extending to the top, is generally of good quality. The columns have an average height of a few microns, but some extend to the top surface of the film and show up as pits of a hexagonal shape. Our results illustrate that by using a lower growth rate the extent of the columnar region can be significantly reduced, although it cannot be completely avoided in such a highly mismatched system without using a buffer [3].

We interpret the image contrast between the individual columns and the surrounding uniform film as due to the increased radiative efficiency due to high electron concentration. Using spatially resolved CL spectroscopy and Raman spectroscopy, we found that the hexagonal pits and the bright interface columnar region are responsible for the high residual free-carrier concentration in the layers, typically higher than (3–4) $\times$ 10^{18} cm^{-3} [4, 5]. The incorporation of residual impurities, i.e. O or/and Si, might be due to a change in relative energies and growth rates of different crystal planes. In most of our films grown without a buffer on the top surface of the film, spatially resolved SIMS imaging identified nonuniformities of in-plane oxygen distribution with oxygen concentration significantly increasing at surface hexagonal pits.

Further TEM analysis is used to shed light on the nucleation process of the columns. The TEM images taken from the interface region of the same layer, observed by means of CL,

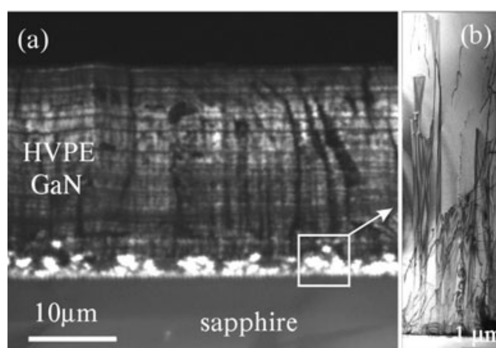

Figure 1. (a) A panchromatic CL image in cross-section of a 30 μm thick HVPE-GaN layer on sapphire. (b) A cross-sectional TEM image of the same layer.

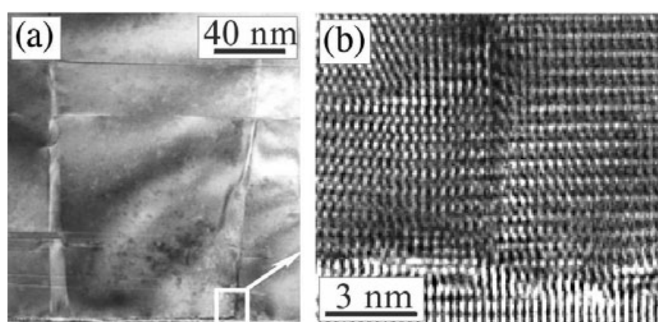

Figure 2. (a) The nucleation region of a columnar domain at the GaN/sapphire interface; (b) a HRTEM image along the $(11\bar{2}0)$ zone axis of the domain boundary.

show isolated columns of a similar inverted pyramidal shape, elongated in the [0001] direction (figure 1(b)). Good-quality material and a few dislocations are observed between them. Two of the six limiting boundaries enclosing the domains are seen. An inclination angle of $\sim 4°$ is estimated between the facets and the normal to the GaN(0001) plane in the TEM image. This is in a very good agreement with the angle of inclination of the boundaries of the bright domains in the CL image (figure 1(a)). The observed angle of inclination permits increase of the domain dimensions from the observed nanometre scale at their base to the micrometre scale at their tops.

Figure 2(a) shows a cross-sectional TEM image of HVPE-GaN grown directly on sapphire imaged down the $[11\bar{2}0]$ zone axis. Errors in hexagonal stacking due to both growth and glide processes are present. Stacking faults (SFs) in the basal planes and stacking mismatch boundaries (SMBs) where two growth domains meet are seen. A higher magnification of one of the SMBs (figure 2(b)) taken in the nucleation region of the domains shows that it originates at the epilayer/substrate interface. The boundary is found to be associated with a substrate bilayer step at the sapphire/GaN layer interface. The SMB arises from the coalescence of two islands that grow on two adjacent terraces on both sides of the step. In the HREM image in figure 2(b) one can also see that the stacking sequence across the boundary is disturbed. The lattice sites from the two sides of the boundary are displaced, forming the SMB. The variety of basal plane SFs and SMBs helps the accommodation of the two lattices of GaN and sapphire. Their density gradually decreases with increasing thickness.

The 3D columnar growth is eliminated in the samples grown on a reactively ion sputtered 500 Å thick AlN buffer and on a MOCVD-GaN template. Thus we can conclude that the large-scale structural defects form because of the 3D growth of islands, followed by coalescence and a transition to a lateral 2D growth with the increase of film thickness. The reason is the high growth rate typical for the HVPE as well as the large misfit. The large-scale defects seem to be typical in highly mismatched GaN heteroepitaxy at high growth rates [6, 7]. However, detailed studies and an explanation of the nature and microstructure of these columnar domains in HVPE-GaN are lacking. The problem has not received a great deal of microstructural analysis because of the difficulty of observing defects, tens or hundreds of micrometres in size, by electron microscopy and drawing a link between the observation of defects on a macroscopical scale (i.e. CL images) and on a microscopical scale (by TEM) in thick layers.

4. Microstructure of thick HVPE-GaN films

The observations described in the previous section gave us a description of the predominant growth mechanism, on which basis the appearance of extended defects of different types becomes clear. The most common microstructural defects in the thick HVPE-GaN films are described and illustrated hereafter.

4.1. Dislocations

In the GaN layers on sapphire, due to the nucleation mechanism, growth-induced dislocations lying on crystallographic planes other than the primary and secondary slip planes, i.e. $\{2\bar{1}\bar{1}0\}$, appear (figure 3(a)). They occur on grain boundaries formed between neighbouring growth domains at their coalescence in order to accommodate the slight misorientation between them. These are the pure-edge type ($\boldsymbol{a}$-type) and make up the majority of the dislocations in GaN. They appear to accommodate the twist misorientation (rotation around the $\boldsymbol{c}$-axis) between growth domains. The tilt misorientation (a small tilt of the $\boldsymbol{c}$-axis) is accommodated by dislocations of a screw component ($\boldsymbol{c}$-, or ($\boldsymbol{a}+\boldsymbol{c}$)-type dislocations) and they appear in lower densities. Although the overall density is reduced over a certain distance from the substrate to the top of the layer, the density still remains high ($\sim 10^8$ cm^{-2}). The reason is the difficulty of dislocation interaction and annihilation, because of the preferred easy glide systems and their low mobility and straight propagating lines parallel to the c-axis growth direction (figure 3(b)). Basal plane dislocations with a Burgers vector $\boldsymbol{b} = (1/3)\langle 11\bar{2}0\rangle$ are also observed (figure 3(a)). A plan-view TEM image (figure 4(a)) shows the arrangement of dislocations in low-angle grain boundaries which are misoriented by a few degrees and delineate subdomains.

Provided that the growth process is optimized by the use of different types of buffer and/or substrate surface pretreatment, a random distribution of the dislocations (figure 4(b)) and a substantial reduction of their density ($\sim 10^7$ cm^{-2}) is achieved. The growth process is no longer 3D island growth, but rather 2D growth with a high lateral-to-vertical growth rate ratio.

4.2. Stacking faults

Planar defects due to a disturbed stacking sequence are observed in our samples lying on different lattice planes of the hexagonal system. Basal plane SFs with the fault plane (0001) and prismatic SFs with the fault plane $(10\bar{1}0)$ or $(11\bar{2}0)$ are seen. SMBs, which were first reported in GaN grown by MBE on SiC [8], are planar faults separating growth domains usually originating from steps on the substrate surface (figure 2(b)).

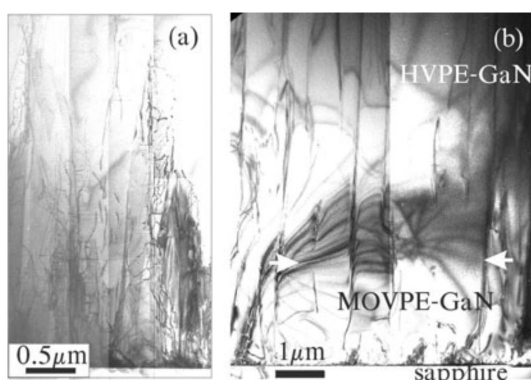

Figure 3. (a) A cross-sectional TEM image of GaN/sapphire and (b) GaN/MOCVD-GaN template/sapphire.

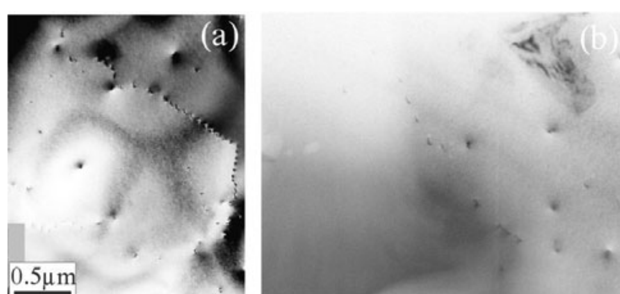

Figure 4. Plan-view TEM images of the HVPE-GaN films showing (a) the arrangement of dislocations in grain boundaries and (b) the random dislocation distribution.

The first ∼200 nm of the near-interface region in figures 2(a), (b) is observed to contain a large density of basal SFs. Errors in hexagonal stacking due to both growth and glide processes are present. They are of intrinsic (type I and type II) or extrinsic character. SFs of 'type I' with a displacement vector $\boldsymbol{R} = (1/6)[2\bar{2}03]$, which are caused by the growth process are observed. 'Type II' SFs with the displacement vector $\boldsymbol{R} = (1/3)[10\bar{1}0]$ that may be caused by a glide process and extrinsic SFs characterized by a displacement vector $\boldsymbol{R} = (1/2)(0001)$ are also observed but of a lower density. The density gradually decreases with thickness. Their formation is attributed to the interface strain because the lattice mismatch can cause a fault in the stacking order of the atomic layers and/or could be due to slip resulting from different thermal contraction during cooling down from the growth temperature.

4.3. Inversion domains

Inversion domains (IDs) embedded in the main wurtzite-GaN matrix and confined to the interfacial area are seen in figure 5. The IDs are tens of nanometres to 100 nm in width and their heights range from ∼1 to several tens of microns. They have six $\{10\bar{1}0\}$ boundaries and a propagation line along the *c*-axis. Two of the six edges of the IDs and also the 'roofs' are seen (figure 5, the inset). The boundaries appear in strong contrast for $g = (0002)$, in weak or no contrast for $g = (10\bar{1}0)$ and the 'roofs' are in contrast for $g = (10\bar{1}1)$.

In HVPE-GaN layers which are known to grow with Ga polarity, the IDs are N polar and terminated along the growth direction by $\{10\bar{1}1\}$ facets; they are called 'house-shaped

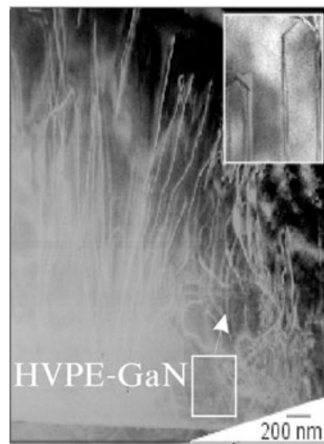

Figure 5. A low-magnification $[11\bar{2}0]$ cross-sectional picture of 50 μm thick GaN with 'house-shaped' IDs. The inset shows a magnified image of the IDs.

domains' [9]. This is explained by assuming that the material inside the domain grows with a lower rate than the surrounding material, according to the difference in growth rate between the (0001) and $(000\bar{1})$ directions.

We should note that we have not observed IDs in our GaN layers grown on MOCVD-GaN templates and on sputtered AlN buffers.

4.4. Nanopipes

A high-magnification plan-view image of the termination of the nanopipe at the surface of the films is shown in figure 6(a), end on. The open core reveals the six close-packed $\{10\bar{1}0\}$ surfaces of a hexagon. In figure 6(b) the nanopipe is imaged tilted at a certain degree to the direction of the electron beam, and the hollow core and the open pit are seen. A Burgers circuit drawn around the hexagons shows the Burgers vector on the (0001) plane to be zero, thus confirming the existence of a screw component.

In the low-magnification plan-view image in figure 6(c), two openings of nanopipes are visible and they are associated with a helical contrast suggesting the nanopipes to be situated in the centres of growth spirals [10]. The TEM images are taken from GaN layers grown on MOCVD templates.

5. Conclusions

Although the defects in GaN generally have a less deleterious effect on optical emission compared to that in other semiconductors, they cause an important scattering mechanism reducing the carrier mobility. We have briefly summarized the most important groups of structural defects in thick HVPE-GaN layers grown directly on sapphire and the effect of the growth on buffers on their behaviour is illuminated. Growing layers on AlN and GaN templates results in improved bulk quality and significantly smoother film surfaces. We found that the growth on templates helps to:

(i) eliminate the large-scale structural defects at the sapphire/GaN interface, which leads to
(ii) a reduction of the concentration and nonuniform distribution of residual carriers; and

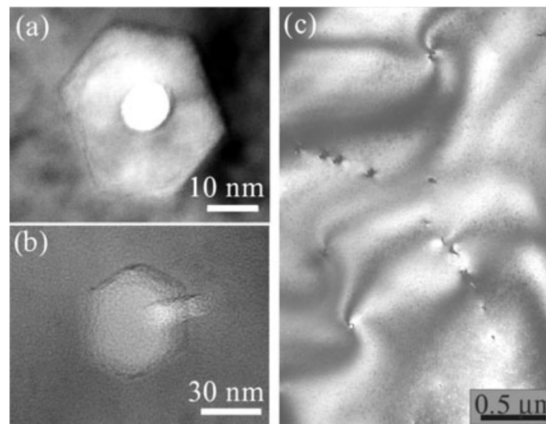

Figure 6. A HRTEM plan-view image (near the [0001] zone) of a typical nanopipe in a 20 μm thick GaN film: (a) the hexagonal opening at the top surface of the film and the empty core viewed end on and (b) inclined to the electron beam; (c) a low-magnification TEM plan-view image. Two openings of nanopipes are seen in the centres of growth spirals.

(iii) good-crystal-quality layers with a lower density of extended defects such as dislocations, SFs and IDs are achieved.

Acknowledgments

The collaboration of P Persson and L Hultman is gratefully acknowledged.

References

[1] Ponce F 1997 Microstructure of epitaxial III–V nitride thin films *GaN and Related Materials* ed S J Pearton (Amsterdam: Gordon and Breach) p 141
[2] Paskova T, Goldys E M and Monemar B 1999 *J. Cryst. Growth* **200** 1
[3] Paskova T, Goldys E M, Yakimova R, Svedberg E B, Henry A and Monemar B 2000 *J. Cryst. Growth* **208** 18
[4] Arnaudov B, Paskova T, Goldys E M, Evtimova S and Monemar B 2001 *J. Appl. Phys.* **64** 45213
[5] Valcheva E, Paskova T, Abrashev M V, Persson P O, Goldys E, Beccard R, Heuken M and Monemar B 2001 *J. Appl. Phys.* **90** 6011
[6] Zhang W, Alves H R, Bläsing J, Hofmann D M, Krost A and Meyer B K 2000 *Proc. IWN2000 (Nagoya) (IPAP Conf. Ser. vol 1)* (Tokyo: The Institute of Pure and Applied Physics) p 46
[7] Hsu J W P, Lang D V, Richter S, Kleiman R N, Sergent A M and Molnar R J 2000 *Appl. Phys. Lett.* **77** 2873
[8] Sverdlov N, Martin G A, Morkoç H and Smith D J 1995 *Appl. Phys. Lett.* **67** 2063
[9] Romano L T, Northrup J E and O'Keefe M A 1996 *Appl. Phys. Lett.* **69** 2394
[10] Qian W, Rohrer G S, Skowronski M, Doverspike K, Rowland L B and Gaskill D K 1995 *Appl. Phys. Lett.* **67** 2284